Materials Science-Poland, 33(1), 2015, pp. 126-130
http://www.materialsscience.pwr.wroc.pl/
DOI: 10.1515/msp-2015-0005

DE GRUYTER OPEN

Phase, microstructure and microwave dielectric properties of A-site deficient (La, Nd)$_{2/3}$TiO$_3$ perovskite ceramics

MUHAMMAD SALEEM[1,2], YASEEN IQBAL[1*], SHAN QIN[2], XIANG WU[2], FENG ZHU[2]

[1]Materials Research Laboratory, Institute of Physics and Electronics, University of Peshawar, 25120, Pakistan
[2]School of Earth and Space Sciences, Peking University, Beijing 100871, China

(La, Nd)$_{2/3}$TiO$_3$ ceramics were prepared through a conventional solid state mixed oxide route. For phase and microstructure analysis, XRD and SEM were used, respectively. Microwave dielectric properties were measured using a network analyzer. XRD patterns revealed the formation of the parent (La, Nd)$_{2/3}$TiO$_3$ phase along with (La, Nd)$_4$Ti$_9$O$_{24}$ as a secondary phase. The microstructure consisted of rectangular and needle shaped grains, which decreased in size from 4 μm to 2 μm with an increase in sintering temperature from 1300 °C to 1350 °C. Decrease in grain size caused an increase in density of the samples from 4.81 g/cm^3 to 5.17 g/cm^3. Microwave dielectric properties of the samples calcined and sintered in air atmosphere were $\varepsilon_r = 40.35$, Q × f = 3499 GHz and $\tau_f = 0$ ppm/°C, whereas for a sample calcined in nitrogen and sintered in air they were $\varepsilon_r = 40.18$, Q × f = 4077 GHz and $\tau_f = +4.9$ ppm/°C, respectively.

Keywords: *A-site deficient perovskites; dielectrics; phase analysis; ceramics*

1. Introduction

Rapid advancement in wireless communication systems became possible due to the advancement in dielectric ceramics used as dielectric resonators [1, 2]. A-site deficient perovskite ceramics, like La$_{2/3}$TiO$_3$, Nd$_{2/3}$TiO$_3$, La(Nd)$_{1/3}$NbO$_3$, Nd$_{1/3}$NbO$_3$, Ca$_{(1-x)}$Nd$_{2x/3}$TiO$_3$ and La$_{1/3}$NbO$_3$, provide a basis for ceramics to be used in telecommunications due to their good dielectric properties, i.e. quality factor higher than 10000 GHz, temperature coefficient of resonant frequency near ±10 ppm/°C and dielectric constant higher than 40 [3–5]. High ε_r insures miniaturization of size of a portable device as the resonant frequency of a resonator is inversely proportional to the square root of dielectric permittivity. High $Q \times f$ determines the selectivity of the signals and near zero TCF ensures the temperature stability of the resonator [6]. A-site deficient perovskites have been studied for their ionic conductivity by several researchers; however, less attention has been given to their dielectric properties [7, 8]. It has been reported that in Li-doped La$_{2/3}$TiO$_3$ ceramics, ionic conductivity is due to Li-ion migration via vacancy formation [9]. In Al-doped La$_{2/3}$TiO$_3$ ceramics, oxide ion conductivity (O^{-2}) is observed at low temperature [10]. Order-disorder transformation of A-site cations/vacancies plays an important role in the determination of electrical properties of A-site deficient perovskites. Ordering in A-site deficient perovskite ceramics can be increased by increasing the number of vacancies [11]. It has been reported that ordering arrangement of A-site cations/vacancies has a positive effect on $Q \times f$ of A-site deficient perovskite ceramics [12]. La$_{2/3}$TiO$_3$ and Nd$_{2/3}$TiO$_3$ are A-site deficient perovskites with one-third of A-site vacant. In La$_{2/3}$TiO$_3$, A(1) sites are fully occupied by La^{+3} cations, whereas A(2) sites are partially occupied by vacancies and La^{+3} ions [7]. La$_{2/3}$TiO$_3$ has a high dielectric constant of 90 with $Q \times f$ greater than 15000 GHZ but with a positive temperature co-efficient of resonant frequency ∼190 ppm/°C [4]. On the other hand, in Nd$_{(2-x)/3}$Li$_x$TiO$_3$ all the compositions with different values of x possess negative temperature coefficient of resonant frequency (−20 ppm/°C to −256 ppm/°C depending on x within $0.0 \leqslant x \leqslant 0.5$) [12]. In this research work a

*E-mail: dryaseeniqbal@yahoo.co.uk

solid solution of La_2O_3, Nd_2O_3 and TiO_3 was prepared in an attempt to get a ceramic material with τ_f close to zero. To the best of our knowledge, no literature exists regarding this composition.

2. Experimental

(La, Nd)$_{2/3}$TiO$_3$ (LNT) ceramic powder was prepared by a solid state mixed oxide route. For this purpose La_2O_3 (99.99 %, Alfa Aesar), Nd_2O_3 (99 %, Alfa Aesar) (where each La and Nd were 50 mol % of the A-site ratio) and TiO_2 (99.9 %, Alfa Aesar) were weighed according to their stoichiometric ratios. The precursor was wet milled with Y-toughened zirconia balls (media) and propanol (lubricant) in polyvinyl jars for 24 h using a benchtop planetary ball mill. The wet milled powder was dried overnight in an oven at ~95 °C and then sieved using a 300 µm mesh. DTA/TGA of the as mix-milled sample was carried out to find the temperature, at which a phase change may occur and to calculate the mass loss during the heat treatment. The as mix-milled sample was then calcined at 1150 °C for 4 h at a heating/cooling rate of 5 °C/min both in air atmosphere and in nitrogen atmosphere, followed by 24 h re-milling. The powder was then pressed into pellets of 10 mm diameter and 5 to 6 mm thickness at 100 MPa. The pellets were then sintered in pairs at 1300 °C, 1325 °C and 1350 °C in the furnace at a heating/cooling rate of 5 °C/min. Densities were measured using Archimedean method with a MD-300s high precession densitometer. Phase determination was performed using a conventional X-ray diffractometer (XPERT-PRO, MPD) with CuKα radiation (λ = 1.5406 Å) operating at 40 mA and 40 kV with a step size $2\theta = 0.0170°$ and scan time of 0.5 sec per step. For scanning electron microscopy (SEM) the samples were ground and polished using "BUEHLER EUTOMET 250" grinder and polisher. The polished samples were thermally etched at temperatures 10 % less than their corresponding sintering temperatures for 30 min at a heating/cooling rate of 10 °C/min and gold-coated to avoid charging in SEM. SEM examination of the samples was performed using a FEI, Quanta, FEG 650 SEM. Energy dispersive spectroscopy was performed using a INCA, Synergy (Oxford) EDS detector. Microwave dielectric properties of the samples calcined both in air and in nitrogen atmosphere at 1150 °C, and sintered at 1350 °C in air, were measured using S-parameter network analyzer (HEWLETT8720ES, 50 MHz to 20 GHz) employing Hakki and Coleman method [13, 14]. Measurement of $Q \times f$ was performed at $TE_{01\delta}$ resonant mode in reflectance, whereas ε_r was measured at TE_{011} resonant mode. τ_f was measured in the temperature range of 20 °C to 80 °C and determined from equation 1:

$$\tau_f = \frac{(f_2 - f_1)}{f_1(T_2 - T_1)} \tag{1}$$

where f_1 and f_2 are resonant frequencies at T_1 and T_2, respectively.

3. Results and discussion

Thermal gravimetric analysis (TGA) and differential thermal analysis (DTA) graphs are shown in Fig. 1. The first portion of the TGA in the temperature range of 30 to 100 °C shows the dehydration of moisture. Major weight loss (4.2 wt.%) occurring in the temperature range from 300 °C to 380 °C, is expected to be due to the dehydration of La_2O_3 [15]. Overall weight loss in the temperature range of 20 °C to 1200 °C was 11.59 wt.%. The weight loss at different temperatures, given in Table 1, may be due to the dehydration of the moisture absorbed by the different oxides. Metal oxides can absorb moisture up to 800 °C, therefore, they are usually heated at 900 °C for several hours prior to weighting [2, 3]. The differential thermal analysis (DTA) showed the beginning of exotherm at 370 °C and a peak at 1132 °C, which may be due to the crystallization of the relevant phase.

Room temperature XRD pattern from (La,Nd)$_{2/3}$TiO$_3$ ceramics sintered at 1350 °C for 4 h at a heating/cooling rate of 5 °C/min, is shown in Fig. 2. The pattern is similar and matched PDF # 49-244 for $Nd_{0.667}TiO_3$ with a slight shifting of the peak positions towards larger d-values due to the incorporation of La with larger ionic radius (1.36Å) for Nd (1.27Å) at A-site of the perovskite structure, which results in an

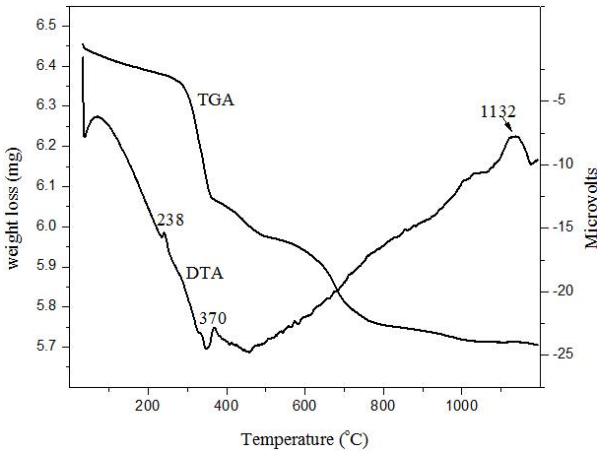

Fig. 1. DTA/TGA graph of LNT as mix-milled sample showing the temperature, at which exothermic reaction takes place and the weight loss occurs during heating process.

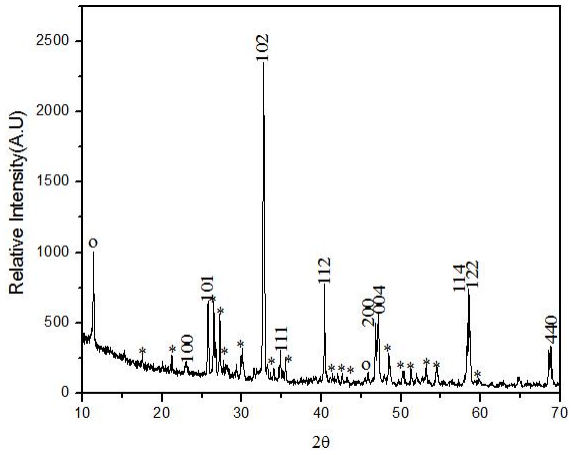

Fig. 2. XRD of the LNT sample sintered at 1350 °C showing the major phase $(La, Nd)_{0.663}TiO_3$. The peaks marked as '*' represent secondary phase $(La,Nd)_4Ti_9O_{24}$ and those marked as '*o*' represent superlattice reflections.

Table 1. The weight loss of LNT ceramics at different temperatures.

S. No.	Temperature range (°C)	Weight loss (mg)	wt. loss (%)
1	20 – 300	0.099737	1.55%
2	300 – 380	0.26546	4.2%
3	380 – 480	0.103599	1.7%
4	440 – 680	0.074127	1.24%
5	680 – 710	0.097476	1.65%
6	710 – 980	0.087038	1.5%
7	980 – 1200	0.021052	0.37%

expansion of unit cell volume [16]. This indicates the formation of the parent $(La, Nd)_{0.667}TiO_3$ phase. Some additional peaks marked as "*" matched PDF # 33-943 for $(La, Nd)_4Ti_9O_{24}$ indicating the formation of a secondary phase [11]. Peaks marked as "*o*" come from superlattice reflections. Superlattice reflections arise from A-site cation/vacancy, ordering which results in the doubling of the perovskite unit cell [12, 17]. The formation of secondary phases in A-site deficient perovskite ceramics, like $La_{2/3}TiO_3$ and $Nd_{2/3}TiO_3$ sintered in air, has been reported in the literature [18].

In the present study maximum density of 5.17 g/cm^3 was achieved for the sample sintered at 1325 °C, which is close to that observed by Huang et al. [18] for La containing compound $Ca_{1-x}La_{2x/3}TiO_3$. Variation of density with sintering temperature is shown in Fig. 3. This increase in density with an increase in temperature is due to the decrease in grain size as a result of increasing sintering temperature. Comparative densities of the samples sintered at different temperatures by different researchers are given in the Table 2.

Fig. 4 shows the secondary electron SEM images (SEI) of $(La, Nd)_{2/3}TiO_3$ ceramics sintered in air atmosphere at 1300 °C, 1325 °C and 1350 °C for 4 h, respectively. The shape of the grains at the surfaces of all the sintered samples resembles plate-late morphology with casually occurring elongated grains, which reflects the presence of two phases. Relatively dense microstructure can be observed for samples sintered at 1350 °C in contrast to those sintered at the other temperatures, which is in agreement with the density results. The microstructure of all the samples is similar to that observed by Bian et al. [11]. Semi-quantitative EDS (Table 3) for the grains labelled as "A" and "B" in Fig. 4a and 4b indicates that the composition of these grains is close to the parent $(La, Nd)_{2/3}TiO_3$ phase. A variation in the grain morphology of polished, thermally etched and gold coated bulk

Table 2. Comparative densities of the compounds containing La and Nd.

Theoretical density (g/cm^3)	Apparent density (g/cm^3)	Phase	Reference
5.25	5.14	$Ca_{1-x}La_{2x/3}TiO_3$	[18]
	5.64	$Ba_{0.86}(Nd_{1.4}Bi_{0.42}La_{0.3})Ti_4O_{12}$	[19]
5.66	5.36	$Sr_{1-x}Ca_xLa_4Ti_5O_{17}$	[3]
	5.17	(La, Nd)$_{0.667}$TiO$_3$ and (La, Nd)$_4$Ti$_9$O$_{24}$	Present work

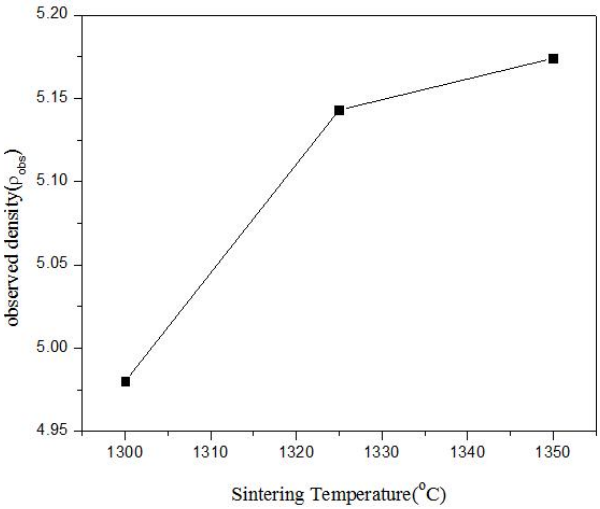

Fig. 3. The plot of apparent density (ρ_{ap}) vs. sintering temperature for (La, Nd)$_{2/3}$TiO$_3$ ceramics showing an increase in ρ_{ap} with increase in sintering temperature from 1300 to 1350 °C.

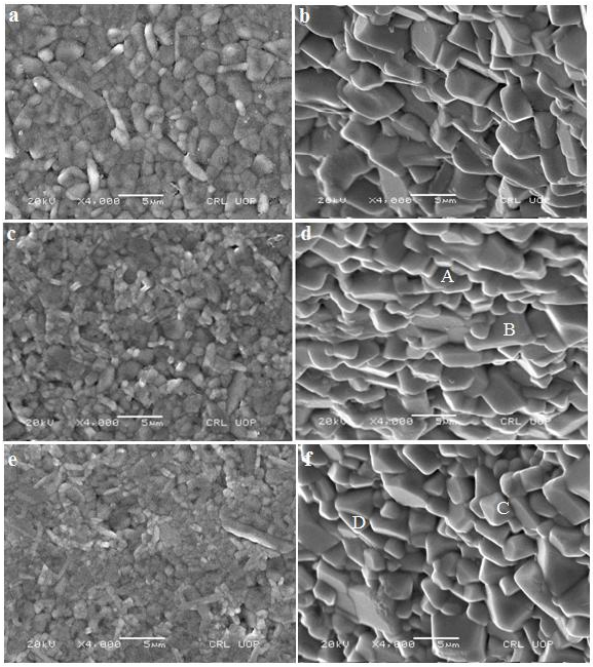

Fig. 4. SEI images of polished and thermally etched bulk samples (a, c, e) and of unpolished and etched surface of LNT ceramics (b, d, f) sintered at 1300 °C, 1325 °C and 1350 °C for 4 h, showing highly dense microstructure and variation in grain morphology at the surface and bulk.

samples can be observed, indicating the formation of a mixture of phases. The semi-quantitative EDS (Table 3) of the grains labeled as "C" indicates that the composition of these grains is close to the parent (La, Nd)$_{2/3}$TiO$_3$ and that of the grains labeled as "D", indicates that the composition of these grains is close to (La, Nd)$_4$Ti$_9$O$_{24}$, which is consistent with the XRD finding. A backscattered electron image of the LNT calcined in nitrogen and sintered in air atmosphere is shown in Fig. 5. The figure shows two different types of grains with cubical and needle shapes, reflecting two different phases.

Microwave dielectric properties of the sample calcined at 1150 °C and sintered at 1350 °C in air atmosphere are $\varepsilon_r = 40.35$, $Q \times f = 3499$ GHz and $\tau_f = 0$ ppm/°C. $Q \times f$ of microwave dielectric ceramics is mainly influenced by grain size, porosity, and secondary phases, which are the main causes of energy losses [2]. τ_f in perovskite ceramics can be related to BO$_6$ octahedra tilting. In A-site deficient perovskite ceramics a number of vacancies exist, which results in the cations/vacancies ordering. This ordering affects the bond length and bond angle that further affects τ_f [20]. Microwave dielectric properties of the sample calcined in nitrogen atmosphere at 1150 °C and sintered at1350 °C in air atmosphere, are

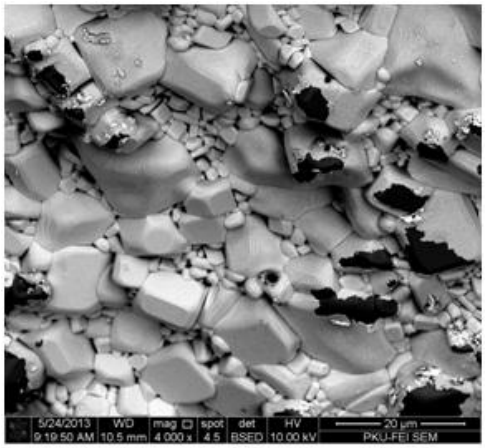

Fig. 5. Backscattered electron SEM image of LNT ceramics calcined in N_2 at 1100 °C and sintered in air atmosphere at 1350 °C, showing two phases.

Table 3. EDS of the different grains.

Grains	La %	Nd %	Ti %
A	29.88	37.97	32.15
B	28.72	36.35	34.92
C	30.12	36.62	33.26
D	25.45	33.94	40.61

$\varepsilon_r = 40.18$, $Q \times f = 4077$ GHz and $\tau_f = +4.9$ ppm/°C. Reducing atmosphere causes a decrease in porosity and grain boundary, which, in turn, causes an increase in $Q \times f$. According to the Clausius-Mossotti equation [21], total dielectric permittivity is proportional to the sum of ionic polarizabilities of the constituent ions, which remains the same after changing the heating environment, thus, no change in dielectric permittivity has been observed.

4. Conclusion

Compositions of $(La, Nd)_{2/3}TiO_3$ (LNT) ceramics were prepared through a conventional solid state mixed oxide route. The samples were characterized by XRD and SEM for phase and microstructural analysis. XRD analysis revealed the formation of $(La, Nd)_{0.667}TiO_3$ as a major phase along with $(La, Nd)_4Ti_9O_{24}$ as a secondary phase. The microstructure consisted of rectangular and needle shaped grains with the sizes ranging from 2 µm to 4 µm upon an increase in the sintering temperature from 1300 °C to 1350 °C. This caused a increase in the ceramics density from 4.81 g/cm^3 to 5.17 g/cm^3. Microwave dielectric properties with $\varepsilon_r = 40.35$, $Q \times f = 3499$ GHz and $\tau_f = 0$ ppm/°C for the samples calcined and sintered in air, were observed, whereas for those calcined in nitrogen atmosphere and sintered in air, $\varepsilon_r = 40.18$, $Q \times f = 4077$ GHz and $\tau_f = +4.9$ ppm/°C were achieved.

References

[1] KIM I.S., JUNG W.H., INAGUMA Y., NAKAMURA T., ITOH M., *Mater. Res. Bull.*, 30 (1995), 307.
[2] IQBAL Y., MANAN A., *J. Mater. Sci.-Mater. El.*, 23 (2012), 536.
[3] IQBAL Y., MANAN A., REANEY I.M., *Mater. Res. Bull.*, 46, (2011), 1092.
[4] AZOUGH F., FREER R., SCHAFFER B., *J. Am. Ceram. Soc.*, 93 (2010), 1237.
[5] KONG Q.D., BIAN J.J., WANG L., GUO Q.H., LIANG Z., *Ferroelectrics*, 407 (2010), 23.
[6] REANEY I.N., IDDLES D., *J. Am. Ceram. Soc.*, 89 (2006), 2063.
[7] BIAN J.J., LI Y.Z., YUAN L.L., *Mater. Chem. Phys.*, 116 (2009), 102.
[8] ZHANG Z., LUMPKIN G.R., HOWARD C.J., KNIGHT K.S., WHITTLE K.R., OSAKA K., *J. Solid State Chem.*, 180 (2007), 1083.
[9] YOSHIOKA H., *J. Am. Ceram. Soc.*, 85 (2002), 1339.
[10] YOSHIOKA H., KIKKAWA S., *J. Mater. Chem.*, 8 (1998), 1821.
[11] BIAN J.J., LI Y.Z., *Mater. Chem. Phys.*, 122 (2010), 617.
[12] BIAN J.J., SONG G.X., YAN K., *Ceram. Int.*, 34 (2008), 893.
[13] HUANG C.L., CHIANG K.H., HUANG C.Y., *Mater. Chem. Phys.*, 90 (2005), 373.
[14] SHEEN J., *Meas. Sci. Technol.*, 20 (2009), 042001.
[15] YADAV B.C., SINGH M., SRIVASTAVA R., DWIVEDI C.D., *Int. J. Green. Nanotechnol.*, 3 (2011), 98.
[16] SHANNON R.D., *J. Appl. Phys.*, 73 (1993), 347.
[17] GUO Q.H., BIAN J.J., WANG L., *J. Am. Ceram. Soc.*, 94 (2011), 172.
[18] HUANG C.L., TSAI J.T., CHEN Y.B., *Mater. Res. Bull.*, 36 (2001), 547.
[19] LIO C.L., LIAN K.H., LIN S.T., *J. Ceram. Process. Res.*, 9 (2008), 562.
[20] PARK H.S., YOON K.H., KIM E.S., *J. Am. Ceram. Soc.*, 84 (2001), 99.
[21] HANNAY J.H., *Eur. J. Phys.*, 4 (1983), 141.

Received 2014-08-07
Accepted 2014-09-30